

Supplemental Materials and Results

Vascular histone deacetylation by pharmacological HDAC inhibition

Short title: Deacetylation by HDAC inhibition

Supplemental Experimental Methods

MTS assay

Cell viability following TSA stimulation was monitored using the CellTiter96® AQueous One Solution Cell Proliferation Assay (Promega). The ability of live cells to induce the reduction of MTS tetrazolium compound (3-(4,5-dimethylthiazol-2-yl)-5-(3-carboxymethoxyphenyl)-2-(4-sulphophenyl)-2H-tetrazolium salt) to a colored formazan product was measured following a 3 hour incubation with CellTiter96® AQueous One Solution Reagent. Absorbance was recorded at $\lambda = 490$ nm.

Crystal violet staining

After TSA stimulation, attached cells were fixed and stained with 0.5% crystal violet (Sigma) in 20% methanol at room temperature. The cells were then washed twice with PBS without $\text{Ca}^{2+}/\text{Mg}^{2+}$ (PBS) and lysis buffer was added (50% ethanol, 0.1 M sodium acetate; 100 μl per well). Following a 10 min incubation the absorbance of incorporated dye was measured at $\lambda = 560$ nm.

Histone extraction protocol

HAECs were stimulated with TSA for 12 hours and then harvested by 10 min incubation at 37°C in PBS containing 1 mM EDTA. Cell pellets were washed twice with ice-cold PBS. Cells were resuspended in AELB (acid extraction lysis buffer: 10 mM HEPES, 1.5 mM MgCl_2 , 10 mM KCl, 0.5 mM DTT and 1.5 mM phenylmethylsulphonyl fluoride) and sulfuric acid was added to a final concentration of 0.26 M. Pellets were incubated on ice for 1 hour with gentle stirring at 10 min intervals. Following centrifugation (13,000 RPM, 10 min, 4°C) the supernatant containing acid soluble proteins was dialysed against 0.1M acetic acid twice for 1 hour followed by overnight dialysis in water. The protein content was determined by Bradford assay.

Protein blotting

Proteins isolated by acid-extraction (2 μg) were resolved by NuPAGE Novex gel (Invitrogen) and transferred to Immobilon-PVDF membrane (Millipore). Blotted membranes were washed twice with Tris buffered saline tween20 (TBST) and blocked in freshly prepared 3% non-fat milk in TBST for 1 hour at room temperature with constant agitation. Membranes were incubated with primary antibodies in freshly prepared 3% BSA solution for 2 hours at room temperature with gentle agitation. PVDF membranes were washed with TBST buffer followed by 1-hour incubation with horseradish-peroxidase-conjugated secondary antibodies (Pharmacia) at room temperature. Protein levels were detected using the ECL chemiluminescence detection system (Sigma). Histone H3 was used as internal loading control.

Monocyte adhesion assay

The human monocyte cell line, U-937, was purchased from ATCC (American Type Culture Collection, (Manassas, VA, USA). Cells were cultured in Roswell Park Memorial Institute (RPMI) 1640 medium (Gibco) containing 10% FBS and antibiotics (penicillin, streptomycin). Primary HAECs grown on 48-well plates (50,000 cells/well) were stimulated with lipopolysaccharide (LPS, 20 mg/ml) or TSA (500 nM) before adding LPS (20 mg/ml) for a further 6 hours. Cells were then washed with PBS and fresh medium containing U-937 cells (5×10^5 cells/ml) added. This was followed by 1 hr incubation at room temperature on a rocking plate. Non-adherent monocytes were washed and adherent cells fixed in 1% glutaraldehyde in PBS prior to image acquisition using an inverted microscope for counting.

TNF stimulation

HAECs were stimulated with 500 nM TSA, TNF (10 ng/ml), or a combination of TNF and TSA for 6 or 12 hours. RNA extraction, cDNA generation and qRT-PCR were performed.

Cytokine and chemokine release assay

Cytokine and chemokine release assays were performed using the Proteome Profiler Human Cytokine Array Kit, Panel A (ARY005, R&D Systems, Minneapolis, US), according to the manufacturers instructions. HAECs (1 million per sample) were stimulated with 500 nM TSA for 12 hours.

PMA

HAECs were seeded onto 96 well plates (20,000 cells per well). After 24 hours, cells were stimulated with TSA (200-1000 nM) for 6 hours followed by 100 ng/ml phorbol 12-myristate 13-acetate (PMA) for 1 hour. The production of reactive oxygen species was monitored by measuring carboxy-H2DFF-DA oxidation (excitation = 495 nm; emission = 520 nm).

Quantitative Reverse Transcriptase-PCR (qRT-PCR)

PCR amplification was performed using a 7500 Fast Real-Time PCR System (Applied Biosystems). cDNA was synthesized using High-Capacity cDNA Reverse Transcription Kit following manufacturers protocol (Applied Biosystems). 5 pmoles of forward and reverse primer, cDNA template and FAST SYBR® Green Master Mix (Roche) were mixed to a final volume of 20 μ l. Reactions were incubated at 95°C for 10 min, followed by 40 cycles of 95°C for 10 s and 60°C for 30 s. Changes in gene expression were determined by normalizing against *HPRT1*.

The primers used for gene expression validation were;

CXCL1, F:CGCAGCAGGAGCGTCCGT, R:TGGGGTCCGGGGACTTCAC;

GCLC, F:GGAAACCAAGCGCCATGCCG, R:ATTCCACCTCATGCCCACT;

HPRT1, F:TGACACTGGCAAAACAATGCA, R:GGTCCTTTCACCAAGCAAGCT;

IL6, F:TCCACAAGCGCCTCGGTCC, R:GTGGCTGTCTGTGTGGGGCG;

IL8, F:TGCAGCTCTGTGTGAAGGTGC, R:TGTGTTGGCGCAGTGTGGTCC;

CCL2, F:AGCAAGTGTCCAAAGAAGC, R:TGGAATCCTGAACCCACTTC;

MIF, F:CGCATCAGCCGGACAGGGT, R:CAGACAGCGTGGTCCCTGC;

NOS3, F:ATGGAGAGAGCTTGCAGCTGCC, R:AGGACACCAGTGGGTCTGAGCA;

NOX4, F:CTCCTTCTCGGTCCGGCGGG, R:GCCAGATGAACAGGCAGAGGTGT;

SERPINE1, F:GGCCCACCTGGCCTCAGACT, R:CAACACCGAGGCCACCCAT;

PRDX1, F:GGGAAAGTGTGCCAGCTGG, R:GCCAGCGCTCACTCTGCT;

CXCL12, F:CACATGGGAGCCGGTCTGC, R:TGCTCGGGATGAGGGCTGGG;

SOD2, F:CAGTGTGCGGCACCAGCAGG, R:TGAGGTTCCAGGGCGCCGTA;

STC1, F:CACTCAGGGAAAAGCATTGCT, R:TGCTGTAGCACTCTCCTGC;

TNFSF9, F:CAAAATGTTCTGCTGATCGATGG, R:CGCCGCAGCTCTAGTTGAA;

NEFH, F:CTACCAGGAAGCCATTCAAGCA, R:AATTGGGCCAAAGCCAATCC;

PALMD, F:GCGGATTCTCCCTGCTTCT, R:TCTTTATCTGTGATGGCCTGGA;
BMX, F:GTGTTGGGGCACTGAGTAA, R:TATCATCCGTCTCAGCTTGTCC;
STAC2, F:ATGAGCGAGAAGGAGAACGA, R:CTTCGGAGGATGGTCTTGAG;
B4GALNT4, F:ATCTCGAGCCTGGAGAACG, R:GGTACACAAATTGCAGGCC;
BMP8B, F:CAGGCTGATCACCAAAGTCA, R:GTTCCGAGAACAGCAGAGG;
H2AFV, F:TCACAGAGAGCTGGGCTACA, R:TCCAACCTTCATCACCACG;
IRS2, F:TCCCACCACTGAAGGAGGCCA, R:CGGGCTGAAACAGTGCTGAGCG;
MECP2, F:ACTCCCCAGAACATACACCTTGCTT, R:TGAGGCCCTGGAGGTCT;
BRM, F:GACGGCTCTCAACTCCAAAGCATA, R:GACGGCGTTCCCTCTCCTGC;
BRG1, F:CCTCTCTCAACGCTGTCCAAGT, R:ATCTGGCGAGGATGTGCTTGTCT.

The primers were used for validation of acetylation by ChIP;

STAC2, F:ACGAAGACCAGTGGCCGCCT, R:CGATCACACCGGCACCGCA;
B4GALNT4, F:CCCCCTCTGCAGGCTCCTCT, R:TATGCCTCCGCCCTCCTG;
NEFH, F:GCCCTCTCCTACACCCCGCA, R:GGTCCTGACCCACCCCCACG;
BMP8B, F:GGCAGCCCAGGTGGCAAAG, R:CTGCCTTCACCCCTGCCCAA;
VCAMI, F:ATTCACTCCGCGGTATCTG, R:CCAAGGATCACGACCATCTT;
IL6, F:TGCACTTTCCCCCTAGTTG, R:TCATGGAAAATCCCACATT;
NOS3, F:GTGAGATGCCAGTGCTGTA, R:ACCTCCCAGTTCTCACACG;
NOX4, F:TGCACGCTCAGAGAACATGAAT, R:CTGTGTCTGGAGGAGCTG;
CCL2, F:CAGCTCTGGAACACACTCA, R:GAGTCACCGTCTGGAAAGC;
GCLM, F:AAGGAAGCGAGAGATGTGGA, R:TCGGTGCTTAAGGCTGGTAG;
PRDX1, F:GTAAAGGCTGCTGGATTCA, R:GAGTTAGCGATGAGCCAAA;
SOD2, F:GTGCTTCTCGTCTTCAGCA, R:CCGTAGTCGTAGGGCAGGT;
GCLC, F:GGTTTCCCCCTCATTCCAT, R:GCAGCAGGCCTACTAGGAAA;
CAT, F:CGCAGGTACACTCTGTGCTC, R:TTCGGCGAATGTAAAAGTCC;
PRDX2, F:CCCTGGGCTGGTTACTTT, R:GCCCTTCTTCTGTCT;
STCI, F:TTGCAGAACGACTGATCACC, R:AAGCCAGGAGAGGGAAAGAG;
TNFSF9, F:CCCAGGGACACCTGTTCTAC, R:GGGGGTCCAAAAGAACTGT;
PALMD, F:GTGCAAAGAGCGGATTCTC, R:CTGGAGTCTCCCTCACCA;
BMX, F:AAGTGTGAGCGTGGTTCC, R:GGCTGTCTGTTCCAGAAG.

Computational Methods

Promoter-specific H3K9/14ac and H3K4me3

In addition to peak calling using MACS, promoter-specific changes associated with H3K9/14ac and H3K4me3 were also determined (Figure 3A and 3B, Supplemental Figure 6E and 6F, Supplemental Figure 7D and 7E). The raw number of reads were counted using BEDTools multicov (Quinlan and Hall 2010) for H3K9/14ac and H3K4me3 at gene promoters (defined as 2.5 kb either side of the TSS, transcription start site).

EdgeR

Where edgeR was used to determine changes in mRNA expression and histone modifications, the following parameters were used: non-differential contig count quantile threshold of 0.3, prior.n of 20 and P value threshold for false discovery rate (FDR) filtering for family wise error rate control of 0.05. Fold changes were reported as the log2 of the fold change (log2FC). EdgeR also reports the logConcentration, a measure of average read abundance across all samples for each gene (RNA-seq) or genomic region (ChIP-seq). The smaller the number, the lower the relative read abundance for that gene or genomic regions, e.g. a gene with a logConcentration of -23 would have a much lower read abundance than a gene with the logConcentration of -13. In Supplemental Figures 6A and 6B, logCPM is used instead of logConcentration. The logCPM is the log2 of the average counts per million reads for all samples.

MA plots and quadrant division

MA plots were generated using a scatterplot of the log2FC versus the logConcentration (or logCPM), based on the results of the edgeR output for RNA-seq, ChIP-seq and CpG-seq. MA plot quadrants, including results shown in Supplementary Table 1, were defined as:

- Upper-left (Q1): genes or regions with a logConcentration of less than -17 (low read/tag counts) and a log2FC > 0.
- Upper-right (Q2): genes or regions with a logConcentration of greater than -17 (high read/tag counts) and a log2FC > 0.
- Lower-left (Q3): genes or regions with a logConcentration of less than -17 (low read/tag counts) and a log2FC of < 0.
- Lower-right (Q4): genes or regions with a logConcentration of greater than -17 (high read/tag counts) and a log2FC of < 0.

Integration of datasets

RNA-seq, ChIP-seq and CpG-seq datasets were integrated using the closestBed function in BEDTools (Quinlan and Hall 2010). Differential H3K9/14ac, H3K4me3 (adjusted $P < 0.05$, based on edgeR output) and DNA methylation were assigned to gene promoters (2.5 kb either side of the TSS).

Distribution of peaks identified at genomic features

Differential and non-differential histone marks were assigned to genomic features. Data were divided into differential histone modifications (adjusted $P < 0.05$) and non-differential histone modifications (adjusted $P > 0.05$, down-sampled to match the size of the differential changes). The number of histone modifications at each feature was counted and Fisher's exact test was used to compare the enrichment of differential versus non-differential changes. The results are reported as the log2 of the odds ratio (Figures 1D and 1E). Bed files of genomic features (both hg19 and mm9) were derived from the UCSC table browser. The promoter region was defined as 2.5 kb either side of the TSS. mRNA transcripts were defined using RefSeq IDs beginning with NM. Non-coding RNA (ncRNA) includes all RefSeq gene transcripts that begin with NR. All other specific ncRNA bed files were downloaded directly from the UCSC browser. These include long ncRNA (lncRNA), transfer RNA (tRNA), microRNA (miRNA) and small nucleolar RNA (snoRNA). This method was also used to determine associations between DNA methylation and changes in mRNA expression as well as H3K9/14ac in response to TSA stimulation (Figures 2A and 2B).

Correlation between TSA and SAHA datasets

To determine the correlation between the TSA and SAHA datasets for gene expression and promoter-specific H3K9/14ac and H3K4me3, Pearson product-moment correlation coefficient (r) was calculated. To visualize the correlation between datasets the log2FC of TSA was plotted against the log2FC of SAHA.

Visualization of changes in H3K9/14ac at the gene promoter

Reads aligned to the promoter (2.5 kb either side of the TSS) were extracted from the bam file using the view option in SAMtools (Li et al. 2009). Using R, localisation of the reads was adjusted by shifting the position of each tag 100 bp to the center of the read (based on the average read size of 200 bp). Kernel density estimation plots were generated in R using a relative library size weighted rectangular kernel with a fixed bandwidth of 200.

Gene Set Enrichment Analysis

Pathway analysis was performed using Gene Set Enrichment Analysis (GSEA) using default parameters (Subramanian et al. 2005).

Identifying ChIP-seq based transcription factor targets

GSEA was used to determine whether promoter-specific changes in H3K9/14ac induced by TSA and SAHA in HAECS were associated with known chromatin associated protein and transcription factor binding sites using ChIP-seq datasets from the ENCODE project¹ (Raney et al. 2011). A catalogue of gene lists (gmt file format for use in GSEA) was generated from the ENCODE ChIP-seq datasets. We identified target genes with ENCODE chromatin associated proteins and transcription factors binding within 3 kb of the TSS. Promoter-specific changes in H3K9/14ac conferred by TSA or SAHA stimulation were pre-ranked before running GSEA by scaling (using the scale function in R) the product of the negative log2 of the adjusted P value and the sign of the fold change (determined by edgeR). Default GSEA parameters were used, except for the number of permutations (10,000). Associations identified by GSEA were defined significant if P value < 0.05 and FDR < 0.05 .

ENCODE¹

<ftp://hgdownload.cse.ucsc.edu/apache/htdocs/goldenpath/hg19/encodeDCC/wgEncodeRegTfbsClustered/>

Cell lines are presented as numbers in Figure 3A-B and Supplementary Figure 7D-E.

| Number | Corresponding cell line |
|--------|-------------------------|
| 0 | GM12878 |
| 2 | HeLa-S3 |
| 3 | HepG2 |
| 8 | K562 |
| 27 | PANC-1 |
| 31 | T-47D+Genistein_100nM |
| 50 | HepG2+forskolin |
| 58 | K562b |

Analysis of the CD4+ T-cell study

Datasets were downloaded from Gene Expression Omnibus (GEO) in fastq format from the series GSE15735 (Wang et al. 2009).

| GEO Sample ID | Sample Name |
|---------------|---------------------|
| GSM393945 | CD4-CBP |
| GSM393946 | CD4-p300 |
| GSM393947 | CD4-PCAF |
| GSM393948 | CD4-MOF |
| GSM393949 | CD4-Tip60 |
| GSM393956 | Act-CD4-Tip60 |
| GSM393957 | Act-CD4-HDAC6 |
| GSM393958 | CD4-H3K9ac-HDACi-0h |
| GSM393959 | CD4-H3K9ac-HDACi-2h |
| GSM393960 | CD4-H3K9ac-HDACi-8h |
| GSM393966 | CD4-PolII-HDACi-0h |
| GSM393967 | CD4-PolII-HDACi-2h |
| GSM393968 | CD4-PolII-HDACi-12h |

Fastq files were converted to fastqsanger format using FASTQ Groomer (Blankenberg et al. 2010) and aligned to hg19 reference genome with BWA (version 0.6.1) using default parameters (Li and Durbin 2009). A count matrix for all samples was created using reads located within 2.5 kb either side of the TSS for all genes. DESeq (using default parameters) was used to determine differential changes in PolII binding and differential acetylation. PolII binding was used as a proxy for gene expression. Due to lack of replicates in that dataset, a rank was determined using the *P* value. To rank ChIP-seq results, the negative log₂ of the *P* value was multiplied by the sign of the fold change. This rank was then used to plot a heat map of PolII and histone acetylation binding at gene promoters.

To determine the association between acetylation and HAT binding in native T-cells, bed files of ChIP-seq data for five different HATs were obtained and converted into gene sets (gmt files) containing the top 500 strongest signals located within 1000 bp of RefSeq genes. GSEA was used (default parameters) to determine whether changes in acetylation were enriched at genes that are associated with HAT binding.

| GEO Sample ID | Sample Name | Bed file |
|---------------|-------------|--------------------------------|
| GSM393945 | CD4-CBP | GSM393945_CD4-CBP_islands.bed |
| GSM393946 | CD4-p300 | GSM393946_CD4-p300_islands.bed |
| GSM393947 | CD4-PCAF | GSM393947_CD4-PCAF_islands.bed |

| | | |
|-----------|-----------|---------------------------------|
| GSM393948 | CD4-MOF | GSM393948_CD4-MOF_islands.bed |
| GSM393949 | CD4-Tip60 | GSM393949_CD4-Tip60_islands.bed |

H3K9/14ac peak calling derived from mouse left ventricle

ChIP-seq data was aligned to mm9. Differential peaks were determined using MACS by directly comparing control samples with TSA stimulation. Peaks with $P = 10^{-5}$ cut-off as determined by MACS were considered significant and used for downstream analyses. Peaks were assigned to a gene if the overlapping sequence was at least 1 bp. Peaks were assigned to a gene promoter if they are within 2.5 kb of the TSS.

Heat map generation

Performed in R using the tool heatmap.2 from the gplots package (<http://CRAN.R-project.org/package=gplots>) with Z-score normalization.

Ideogram generation

Bioconductor package quantsmooth was used in R to generate and visualize genome profiles (Rippe et al. 2012).

Supplemental Table 1. Number of changes in mRNA expression and chromatin modifications in TSA stimulated HAECS.

| Quadrant | mRNA* | differential TSA regions | | | |
|----------|-------|--------------------------|---------|---------|------|
| | | H3K9/14ac | H3K4me3 | H3K9me3 | CpGm |
| 1 | 2979 | 19032 | 526 | 1 | nc |
| 2 | 3107 | 3729 | 2112 | 388 | nc |
| 3 | 1698 | 7376 | 339 | nc** | nc |
| 4 | 3603 | 16585 | 152 | 597 | nc |

*number of differential genes, **no change.

Supplemental Table 2. GSEA of RNA-seq identifies major pathways altered by TSA.

| GSEA gene sets | NES | NOM P value | FDR q value | FWER P value |
|--|-------|-------------------|-------------|--------------|
| Upregulated gene sets | | | | |
| REST | 1.84 | <10 ⁻⁴ | <0.001 | <0.001 |
| Ion channel activity | 1.83 | <10 ⁻⁴ | <0.001 | <0.001 |
| Cation channel activity | 1.83 | <10 ⁻⁴ | <0.001 | <0.001 |
| Cation transmembrane transporter activity | 1.83 | <10 ⁻⁴ | <0.001 | <0.001 |
| Metal ion transmembrane transporter activity | 1.81 | <10 ⁻⁴ | <0.001 | <0.001 |
| Substrate specific channel activity | 1.80 | <10 ⁻⁴ | <0.001 | <0.001 |
| Gated channel activity | 1.79 | <10 ⁻⁴ | <0.001 | <0.001 |
| Downregulated gene sets | | | | |
| Chromatin binding | -2.01 | <10 ⁻⁴ | 0.01 | 0.01 |
| Structure specific DNA binding | -1.90 | <10 ⁻⁴ | 0.07 | 0.07 |
| Cytokine production | -1.89 | <10 ⁻⁴ | 0.06 | 0.08 |
| Negative regulation of biosynthetic process | -1.87 | <10 ⁻⁴ | 0.06 | 0.11 |
| Reactome mitotic M M G1 phases | -1.86 | <10 ⁻⁴ | 0.06 | 0.13 |
| Negative regulation of cellular biosynthetic process | -1.86 | <10 ⁻⁴ | 0.05 | 0.13 |
| Double stranded DNA binding | -1.84 | <10 ⁻⁴ | 0.06 | 0.18 |
| Single stranded DNA binding | -1.83 | <10 ⁻⁴ | 0.06 | 0.19 |

NES (normalised enrichment score), NOM (nominal), FDR (false discovery rate), FWER (family wise error rate).

Supplemental Table 3. RNA-seq identifies major pathways altered by SAHA.

| GSEA gene sets | NES | NOM P value | FDR q value | FWER P value |
|--|-------|-------------------|-------------|--------------|
| Upregulated gene sets | | | | |
| Cation transmembrane transporter activity | 1.92 | <10 ⁻⁴ | <0.001 | <0.001 |
| Metal ion transmembrane transporter activity | 1.92 | <10 ⁻⁴ | <0.001 | <0.001 |
| Reactome neuronal system | 1.92 | <10 ⁻⁴ | <0.001 | <0.001 |
| Cation channel activity | 1.90 | <10 ⁻⁴ | <0.001 | <0.001 |
| Reactome potassium channels | 1.89 | <10 ⁻⁴ | <0.001 | <0.001 |
| Gated channel activity | 1.89 | <10 ⁻⁴ | <0.001 | <0.001 |
| REST | 1.89 | <10 ⁻⁴ | <0.001 | <0.001 |
| Ion channel activity | 1.87 | <10 ⁻⁴ | <0.001 | <0.001 |
| Downregulated gene sets | | | | |
| Chromosomal part | -1.96 | <10 ⁻⁴ | 0.02 | 0.01 |
| Reactome mitotic M M G1 phases | -1.95 | <10 ⁻⁴ | 0.01 | 0.01 |
| Reactome G2 M checkpoints | -1.95 | <10 ⁻⁴ | 0.01 | 0.01 |
| Chromatin binding | -1.91 | <10 ⁻⁴ | 0.01 | 0.03 |
| Reactome regulation of mitotic cell cycle | -1.90 | <10 ⁻⁴ | 0.02 | 0.05 |
| Reactome DNA replication | -1.90 | <10 ⁻⁴ | 0.01 | 0.05 |
| E2F | -1.90 | <10 ⁻⁴ | 0.01 | 0.06 |
| Kegg NOD like receptor signalling pathway | -1.88 | <10 ⁻⁴ | 0.02 | 0.08 |

NES (normalised enrichment score), NOM (nominal), FDR (false discovery rate), FWER (family wise error rate).

Supplemental Table 4. Statistical analyses of changes in SAHA stimulated HAECS.

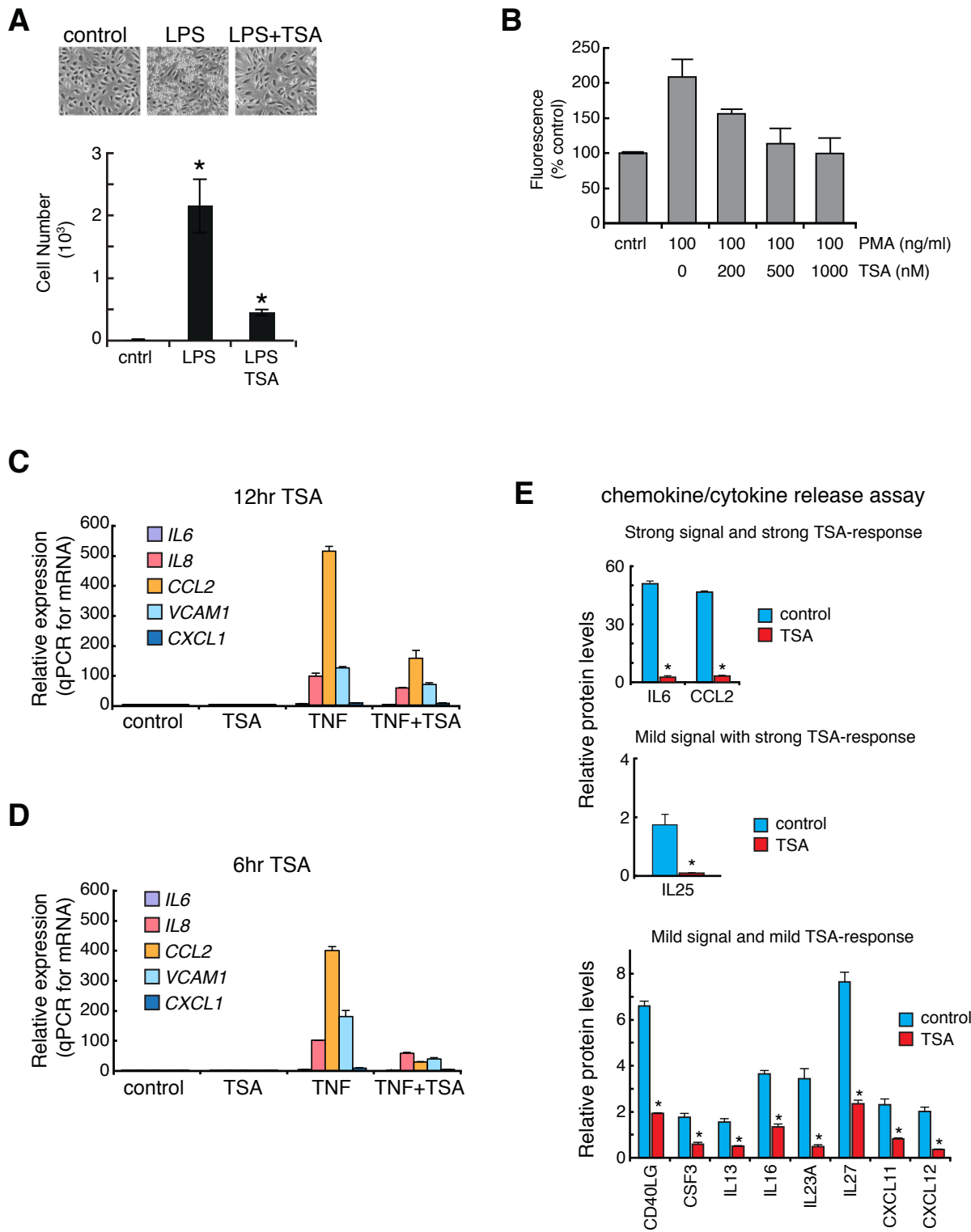
| Histone | P value* | Odds ratio** | increased mRNA expression |
|------------|-------------------------|--------------|--|
| ↑H3K9/14ac | 8.11x10 ⁻⁵⁷ | 2.99 | more likely to occur in up-regulated genes |
| ↓H3K9/14ac | 1.98x10 ⁻³¹ | 0.59 | less likely to occur in up-regulated genes |
| ↑H3K4me3 | 1.28x10 ⁻¹⁴⁰ | 2.27 | more likely to occur in up-regulated genes |
| ↓H3K4me3 | 9.07x10 ⁻⁶ | 0.34 | less likely to occur in up-regulated genes |

| Histone | P value | Odds ratio | decreased mRNA expression |
|------------|------------------------|------------|--|
| ↑H3K9/14ac | 7.42x10 ⁻²⁸ | 0.39 | less likely to occur in down-regulated genes |
| ↓H3K9/14ac | 3.11x10 ⁻¹⁶ | 1.50 | more likely to occur in down-regulated genes |
| ↑H3K4me3 | 1.10x10 ⁻⁸¹ | 0.52 | less likely to occur in down-regulated genes |
| ↓H3K4me3 | 2.59x10 ⁻⁷ | 2.54 | more likely to occur in down-regulated genes |

*calculated using Fisher's exact test to determine correlation of histone modification and gene expression.

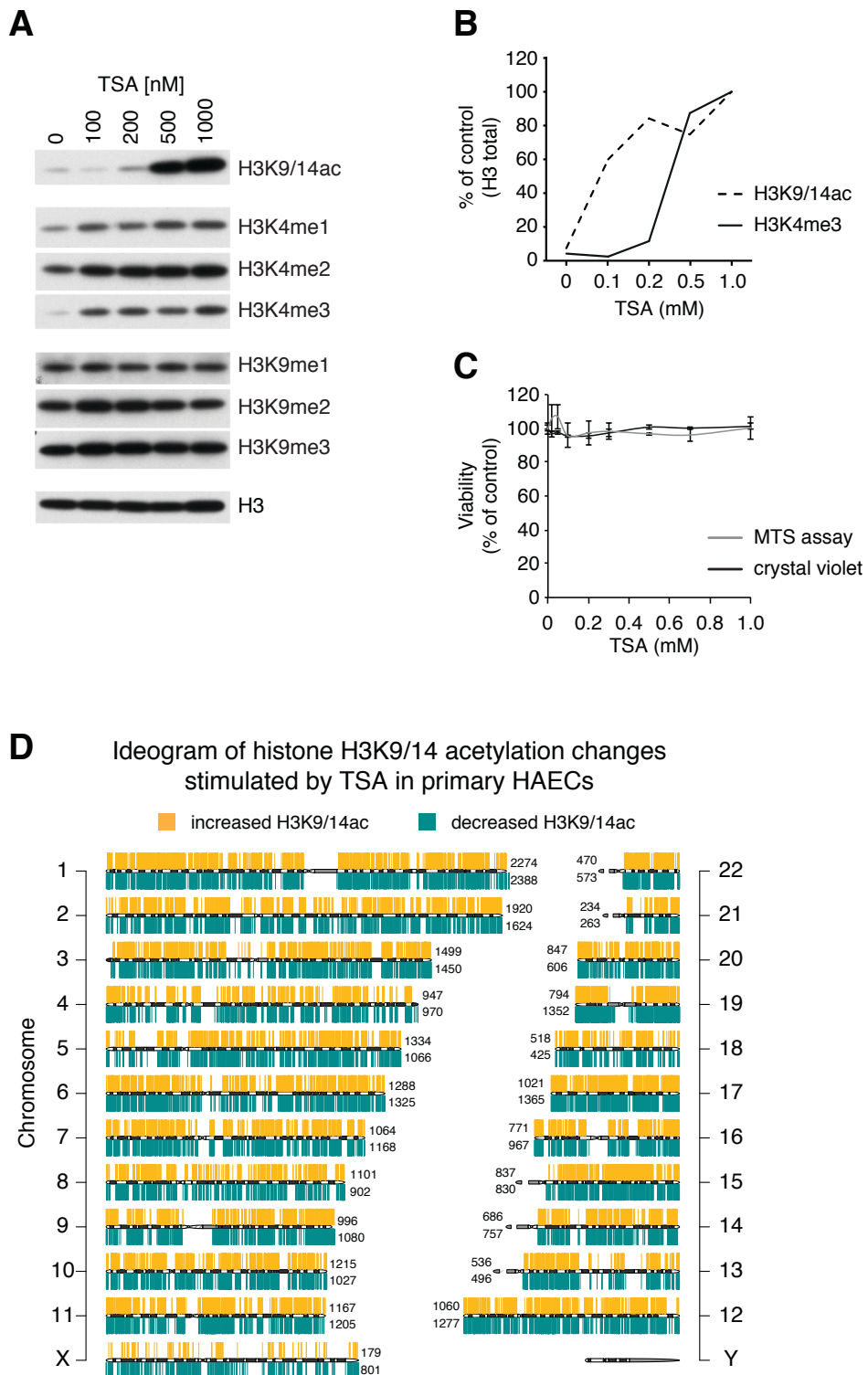
** Fisher's odds ratio <1 indicates gene expression changes that are less likely to be correlated with histone modification.

Supplemental Figure 1



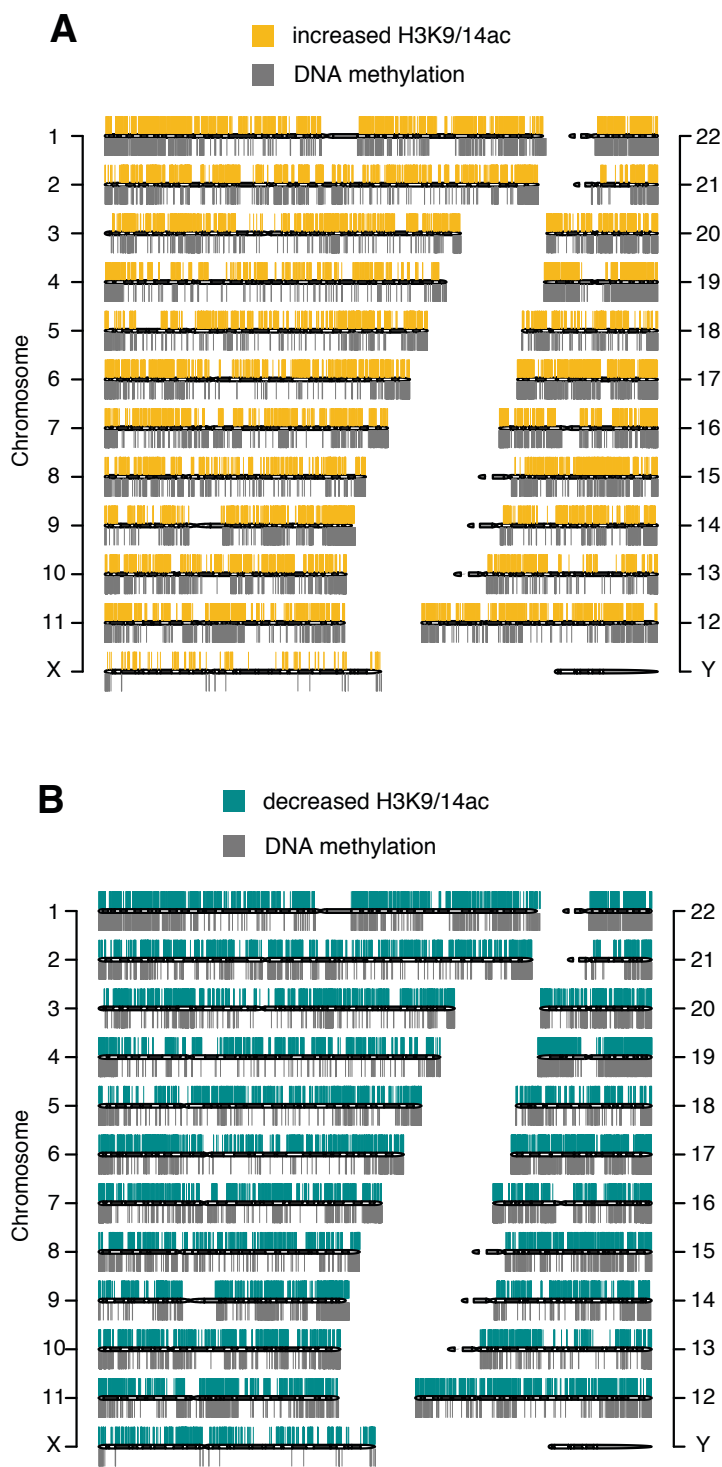
Supplementary Figure 1. TSA prevents inflammatory responses. (A) HAECS were stimulated for 6 hours with 500 nM TSA followed by lipopolysaccharide for 6 hours (LPS, 20 mg/ml). U-937 macrophages (500,000 cells/well) were allowed to adhere to HAECS for 60 minutes and unbound cells washed away. Microscopic view of U-937 adhered to HAECS in the control condition and LPS-stimulated cells in the presence and absence of TSA are shown. The graph depicts the mean values for the numbers of adherent U-937 per microscopic field (n = 3 independent experiments). LPS increased the number of adherent monocytes; *P < 0.05 vs. control. Addition of TSA significantly decreased adhesion of U-937 to HAECS; *P < 0.05 vs. LPS-stimulated cells (unpaired t-test). (B) Stimulation of HAECS for 6 hours with TSA reduces the production of phorbol 12-myristate 13-acetate (PMA)-induced reactive oxygen species (ROS). Fluorescence of carboxy-H2DFF-DA (indicator of ROS) was analyzed 1 hour after protein kinase C (PKC) stimulation with 100 ng/ml PMA. TSA inhibited PMA induced-ROS production. (C-D) TSA attenuates TNF-induced expression of pro-inflammatory cytokines and chemokines as well as adhesion molecule *VCAM1*. HAECS were stimulated with 10 ng/ml TNF for (C) 12 hrs or (D) 6 hrs. (E) Cytokine and chemokine secretion assay reveals an anti-inflammatory profile conferred by TSA. Cell supernatants were assessed for secreted cytokines and chemokines following TSA (500 nM) stimulation of HAECS. Mean values of signal intensities were classified as “strong signal and strong TSA-response”, “mild signal with strong TSA-response” and “mild signal and mild TSA-response”. *P < 0.05, unpaired t-test for all cytokines/chemokines reported. A.U. = arbitrary units. Error bars represent SEM.

Supplemental Figure 2



Supplemental Figure 2. Histone modifications conferred by TSA stimulation in primary HAECs. (A) TSA increases histone acetylation and histone H3K4 methylation. Total histone H3 was used as a loading control. (B) Dose dependent increase in H3K9/14ac and H3K4me3 in TSA stimulated HAECs. Quantitation of histone acetylation and histone methylation signals were compared to unmodified histone H3. (C) Viability of TSA stimulated HAECs was determined using MTS-tetrazolium reduction and crystal violet staining. Data are presented as mean \pm SD, $n = 3$. (D) Ideogram of genome-wide H3K9/14ac distribution (adjusted $P < 0.05$). The proportion of H3K9/14ac regions are indicated beside each chromosome, for example, ChIP-seq identified 2274 acetylated regions and 2388 deacetylated regions were identified on chromosome 1.

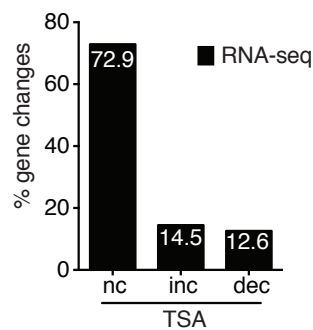
Supplemental Figure 3



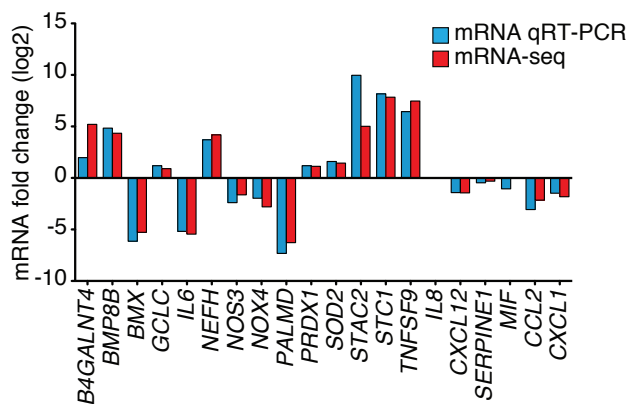
Supplemental Figure 3. DNA methylation is correlated with the action of pharmacological HDAC inhibition at specific genomic regions. Ideograms showing (A) increased H3K9/14ac (yellow) and (B) decreased H3K9/14ac (green) regions relative to DNA methylation (grey).

Supplemental Figure 4

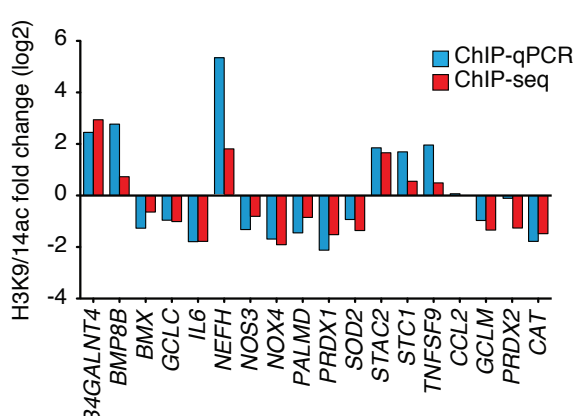
A



B

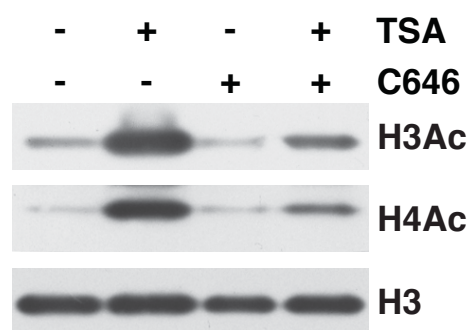


C



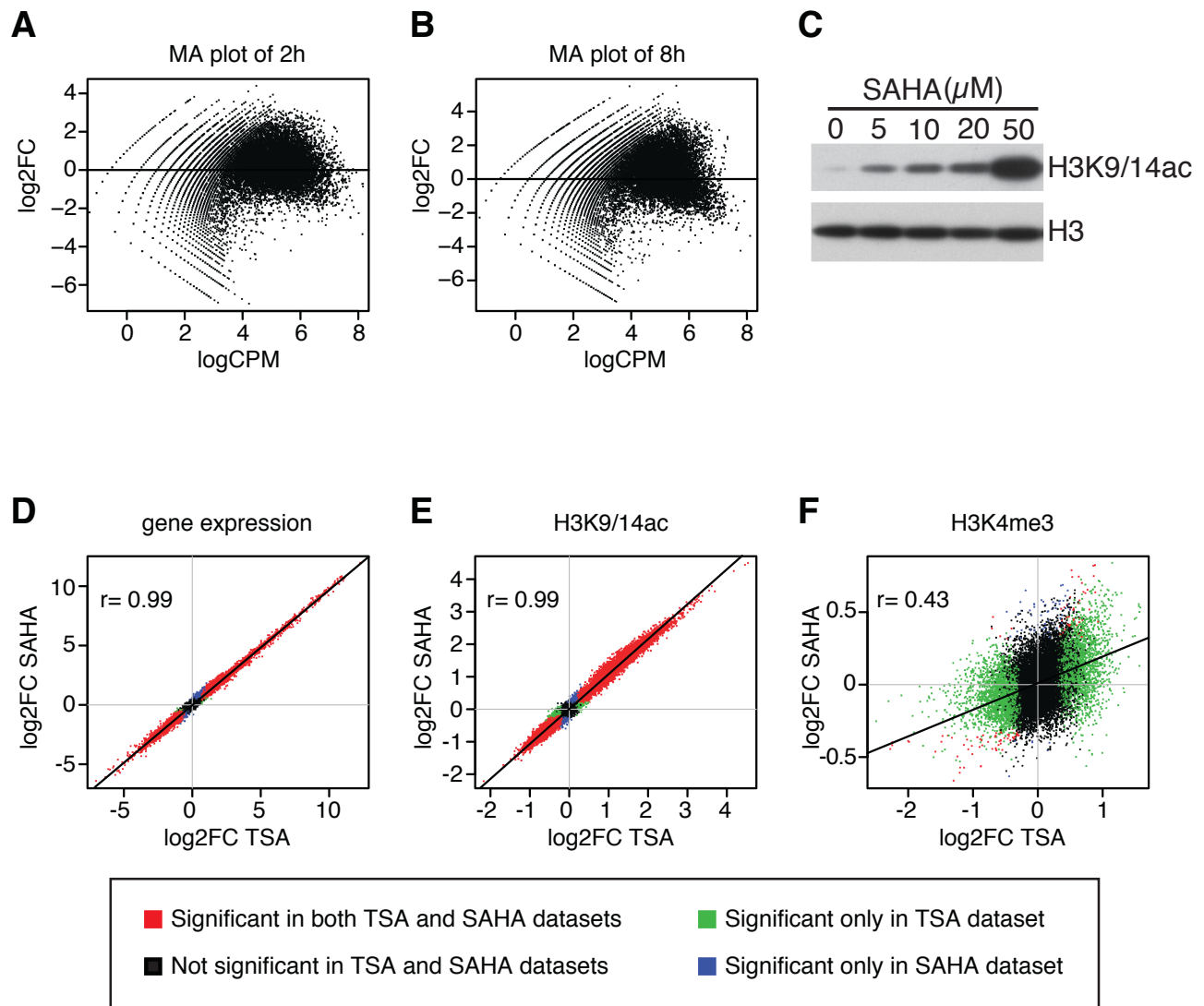
Supplemental Figure 4. Validation of gene expression and H3K9/14ac changes in TSA-stimulated HAECS. Cytokines, chemokines and redox homeostasis were selected for independent experimental confirmation. (A) Shown are the percentage of genes with no significant change (nc) (adjusted $P > 0.05$) as well as genes that were increased (inc) or decreased (dec) in expression (adjusted $P < 0.05$). (B) qRT-PCR validation of mRNA targets derived from RNA-seq, (C) qPCR validation of H3K9/14ac gene targets derived from ChIP-seq experiments.

Supplemental Figure 5



Supplemental Figure 5. Western blot of H3K9/14ac changes derived from HAECs stimulated with TSA (500 nM, 12 hrs), EP300/CREBBP inhibitor C646 (20 μ M, 15 hrs), as well as combined exposure (C646, 20 μ M for 15 hrs and TSA, 500 nM for 12 hrs).

Supplemental Figure 6

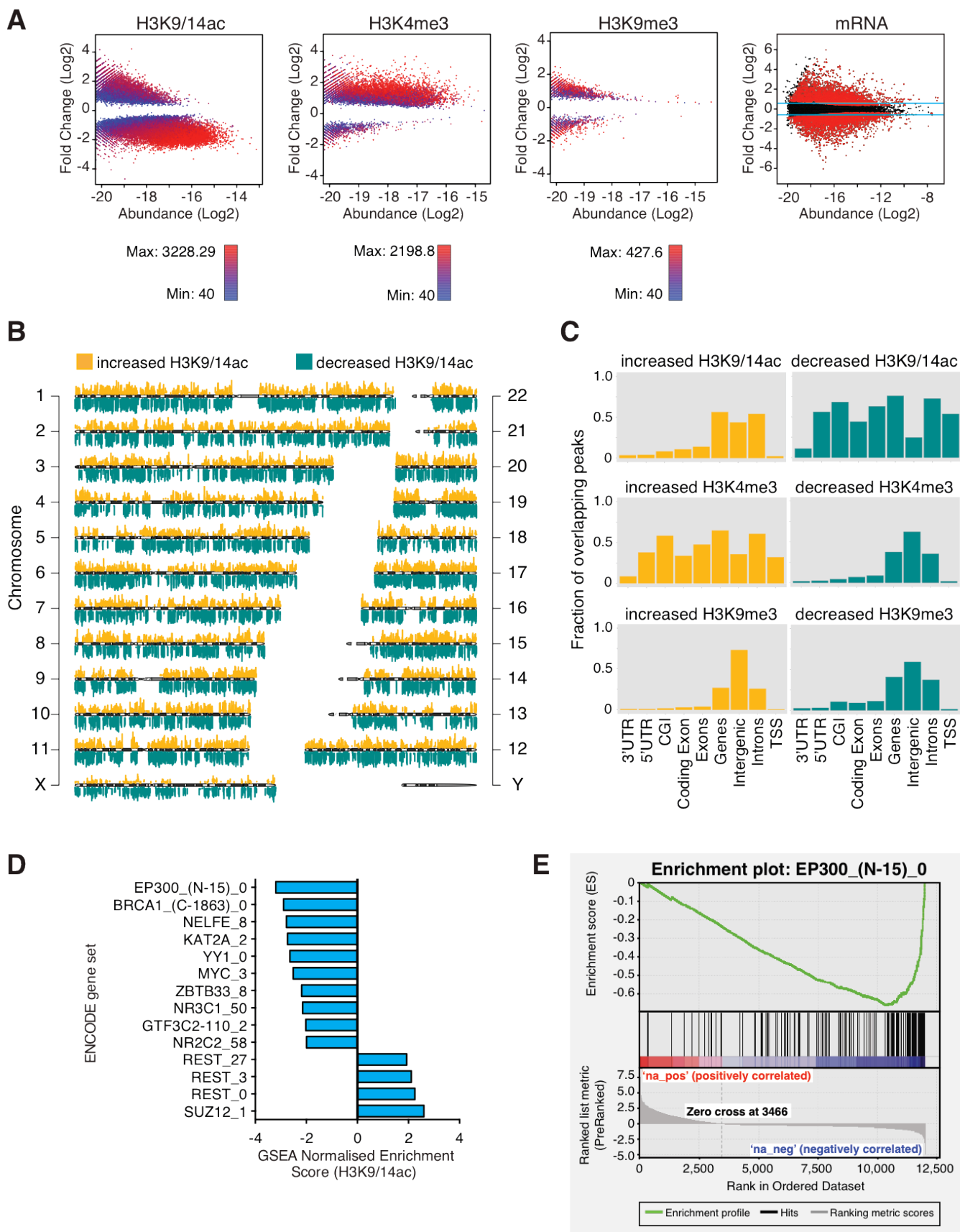


Supplemental Figure 6. H3K9ac changes in CD4+ T-cells stimulated with TSA (100 ng/ml) and sodium butyrate (2 mM) at (A) 2 hrs and (B) 8 hrs. The logCPM is a measure of the concentration of reads (log₂ of the average counts per million for each genomic regions). (C) Western blot of H3K9/14ac changes derived from SAHA stimulated HAECs. Correlation of changes conferred by TSA and SAHA stimulation in HAECs are shown for (D) gene expression, (E) H3K9/14ac and (F) H3K4me3. Only promoter specific changes in H3K9/14ac and H3K4me3 are shown. Pearson's correlation (r) is shown for each plot.

Significant changes in both TSA and SAHA datasets are shown in red and changes observed only in TSA or SAHA datasets are shown in green and blue, respectively (adjusted *P* value < 0.05). Non-significant changes in TSA and SAHA datasets are shown in black.

Supplemental Figure 7

SAHA confers widespread changes in H3K9/14ac of primary HAECS



Supplemental Figure 7. SAHA confers differential histone modification and gene expression changes in primary HAECs. (A) MA plots are shown to visualize the concentration of read counts for differential H3K9/14ac, H3K4me3 and H3K9me3 (color scale corresponding to MACS score) as well as gene expression changes. For mRNA, red represents differential changes (adjusted P value < 0.05) and black represents no change. (B) Genome-wide distribution of differential H3K9/14ac regions in SAHA stimulated HAECs. Differential ChIP-seq regions were determined by MACS. The height of each bar corresponds to the MACS score. (C) Genomic features are represented as increases (yellow) and decreases (green) in H3K9/14ac, H3K4me3 and H3K9me3. (D) GSEA was used to determine enrichment of genes with changes in acetylation (2.5 kb either side of the TSS) in response to SAHA stimulation. Gene sets were derived from the ENCODE TFBS ChIP-seq collection of various transcription factors and chromatin-associated proteins. Negative Normalized Enrichment Score (NES) indicates a correlation of ENCODE derived transcription factor binding sites associated with histone deacetylation. All gene sets are (nominal) $P < 0.05$ and (false discovery rate) FDR q -val < 0.05 . (E) GSEA plot shows H3K9/14ac changes conferred by SAHA at EP300 target genes.

Supplemental References

Blankenberg D, Gordon A, Von Kuster G, Coraor N, Taylor J, Nekrutenko A. 2010. Manipulation of FASTQ data with Galaxy. *Bioinformatics* **26**(14): 1783-1785.

Li H, Durbin R. 2009. Fast and accurate short read alignment with Burrows-Wheeler transform. *Bioinformatics* **25**(14): 1754-1760.

Li H, Handsaker B, Wysoker A, Fennell T, Ruan J, Homer N, Marth G, Abecasis G, Durbin R. 2009. The Sequence Alignment/Map format and SAMtools. *Bioinformatics* **25**(16): 2078-2079.

Quinlan AR, Hall IM. 2010. BEDTools: a flexible suite of utilities for comparing genomic features. *Bioinformatics* **26**(6): 841-842.

Raney BJ, Cline MS, Rosenbloom KR, Dreszer TR, Learned K, Barber GP, Meyer LR, Sloan CA, Malladi VS, Roskin KM et al. 2011. ENCODE whole-genome data in the UCSC genome browser (2011 update). *Nucleic acids research* **39**(Database issue): D871-875.

Rippe RC, Meulman JJ, Eilers PH. 2012. Visualization of genomic changes by segmented smoothing using an L0 penalty. *PloS one* **7**(6): e38230.

Subramanian A, Tamayo P, Mootha VK, Mukherjee S, Ebert BL, Gillette MA, Paulovich A, Pomeroy SL, Golub TR, Lander ES et al. 2005. Gene set enrichment analysis: a knowledge-based approach for interpreting genome-wide expression profiles. *Proc Natl Acad Sci U S A* **102**(43): 15545-15550.

Wang Z, Zang C, Cui K, Schones DE, Barski A, Peng W, Zhao K. 2009. Genome-wide mapping of HATs and HDACs reveals distinct functions in active and inactive genes. *Cell* **138**(5): 1019-1031.